10.1. Introduction

The fast-growing field of soft matter research requires increasingly sophisticated tools for experimental studies. One of the oldest and most widely used tools to study soft matter systems is optical microscopy. Recent advances in optical microscopy techniques have resulted in a vast body of new experimental results and discoveries. New imaging modalities, such as nonlinear optical microscopy techniques that were developed to achieve higher resolution, enable soft matter research at length scales ranging from the molecular to the macroscopic.

The aim of this chapter is to introduce a variety of optical microscopy techniques

usually have smaller WD and vice versa.

Numerical aperture determines important microscope characteristics such as the point spread function (PSF) and, consequently, the resolution. The PSF [Fig. 1(c)] can be thought of as the light intensity distribution in the image acquired by the microscope from a point source, and is given by [1]

$$\mathrm{PSF}(r) = \left[\frac{2J_1(ra)}{ra}\right]^2,$$

where $a = 2\pi\,\mathrm{NA}/\lambda$, J_1 is the Bessel function of the first kind, λ is the wavelength of light and r is the distance from the center of the peak in light intensity [Fig. 1(c)]. In the image plane of a standard optical system, the PSF is shaped as the Airy diffraction pattern with the first minimum at r = W/2 [Fig. 1(d)]. Two Airy discs separated by the distance R Ó W/2 [Fig. 1(d)] can be resolved into separate entities, but not at smaller R [2]. This limit is often called the Rayleigh criterion or the diffraction limit and defines the lateral resolution of the objective as $r_{lateral} = 0.61\lambda/\mathrm{NA}$, i.e., the resolution in the plane orthogonal to the microscope's optical axis. From the definition of $r_{lateral}$ it follows that objectives with higher NA can resolve finer details, however, even for high-NA objectives, the lateral resolution can be only slightly smaller than the wavelength of light used for imaging. Although conventional optical microscopes have poor resolution along the optical axis of a microscope, recently introduced optical imaging techniques, such as confocal and nonlinear optical microscopies, allow for optical imaging with high axial resolution. The axial resolution of an optical system will be introduced later when discussing fluorescence confocal microscopy in section 10.7. Modern imaging

approaches allowing one to overcome the diffraction limit for both radial and axial directions will be discussed in section 10.12.

10.3. Bright field and dark field microscopy

Bright field imaging is perhaps the simplest of all optical microscopy methods. A sample is illuminated by unpolarized white light and the contrast in the image results from direct interaction of the probing light with the sample (absorption, refraction, scattering, reflection, etc.). Figure 2(a) shows a simple schematic diagram of transmission mode (dia-illumination) bright field microscopy, where the illumination light is focused onto the sample by a condenser lens with numerical aperture NA_{cond} and the transmitted light is collected by the objective lens with numerical aperture NA_{obj}. High quality imaging

limitations of bright field imaging is that samples with weak spatial variation of the refractive index or absorption produce images with poor contrast.

Figure 2. Bright field microscopy diagram (a) and textures: (b) toroidal focal conic domains in a smectic liquid crystal (8CB) film spread over a glycerol surface; (c) an array of *P. aeruginosa* cells trapped by an array of infrared laser beams.

Dark field microscopy is a method in which the image is formed by collecting only the light scattered by the sample. All unscattered light coming directly from the illumination source is excluded from the image, thus forming a dark background [Fig. 3(a)]. To achieve this, the specimen is illuminated with a hollow cone of light [Fig. 3(a)] formed by a special condenser with an opaque light-stop blocking the direct light. The oblique illumination light is scattered by objects in the field of view and only the

b)33 -ects iQBTlOects

employed when investigating systems ranging from red blood cells to plasmonic metal

retardation plate or wedge (with known orientation of the optic axis and known phase retardation) and the studied sample. The analysis of the resulting phase retardation patterns yields information complementary to that obtained by imaging the sample between a pair of polarizers alone.

The introduction of a Bertrand lens into the optical train of the microscope enables an imaging mode known as “conoscopy” [Fig. 4(d)]. The Bertrand lens is inserted in the optical train after the analyzer [Fig. 4(a)] and brings the objective’s back aperture plane into the focus. In this arrangement, the sample is illuminated by a strongly convergent cone of light, which provides an interference image [Fig. 4(d)] formed by light passing through the sample at different angles. Conoscopic arrangement of a polarizing microscope allows determination of the type of birefringent materials (i.e., uniaxial or biaxial), orientation of the optic axes, and the sign of birefringence [3, 5].

10.5. Differential interference contrast and phase contrast microscopy

Most common optical microscopy techniques used to enhance the contrast in transparent samples with weak spatial variation of the refractive index are differential interference contrast (DIC) and phase contrast microscopies. In the DIC technique, image contrast results from the gradient of the refractive index within the sample. A sample is placed between crossed polarizers and two beamsplitters, the Nomarski-modified Wollaston prisms [Fig. 5(a)], such that the prisms’ optic axis is kept at 45^{o} with respect to the crossed polarizers. The polarized illumination light is separated by the first beamsplitter into two orthogonally polarized and spatially displaced (sheared) components [red and blue in Fig. 5(a)]. Each component propagates along a different path, giving rise to

diffracted light is collected by the objective and transmitted to the eyepiece through the phase ring, which introduces an additional phase shift to the undeviated reference light. Parts of the sample having different refractive indices appear darker or brighter compared to the uniform background, forming the phase contrast image. Phase contrast imaging is insensitive to polarization and birefringence effects. This is a major advantage when examining living cells and a number of other soft matter systems. Figure 6(b) shows the texture of elongated mycelium hyphae of a common *Aspergillus* mold confined within microfluidic channels [8] obtained with the phase contrast technique.

Figure 6. Phase contrast microscopy: (a) diagram and (b) the image of elongating mycelium hyphae of a common *Aspergillus* mold confined within polydimethylsiloxane-based microfluidic channels (image courtesy of L. Millet).

10.6. Fluorescence microscopy

The optical microscopy techniques described so far are based on transmission, absorption, refraction, or scattering of light. Fluorescence microscopy is a method based on the fluorescence phenomenon, where absorption of light by fluorescent molecules of dyes or fluorophores results in the emission of light at a longer wavelength [Fig. 7(a,b)]. The dye molecules absorb light of a specific wavelengt

or more fluorescent dyes. The excitation wavelength is selected by the excitation filter, reflected by the dichroic mirror to the sample, and is absorbed by the dye molecules in the sample. The fluorescent light emitted by the dye molecules transmits through the dichroic mirror and, after being separated from the excitation light by the emission filter [Fig. 7(c)], is collected by the photodetector. This forms an image with the bright areas corresponding to the sample regions marked with the fluorescent dye and the dark areas corresponding to the regions without the dye [Fig. 7(d)]. A fluorescence microscopy image in Fig. 7(d) shows colloidal structures formed in a nematic liquid crystal by melamine resin microspheres labeled with a fluorescent dye which emits green fluorescence light [9].

10.7. Fluorescence confocal microscopy

A more advanced technique, which offers 3D imaging capability by combining the features of fluorescence and confocal microscopies, is fluorescence confocal microscopy (FCM) shown in Fig. 8. The main feature of confocal microscopy is that the inspection region at a time is a small voxel (volume pixel) and the signal arising from the neighboring region is prevented from reaching the detector by having a pinhole in the detection image plane [Fig. 8(a)]. The inspected voxel and the pinhole are confocal, so that only the light coming from the probed voxel reaches the detector. This enables diffraction-limited imaging resolution not only in the lateral plane but also along the optical axis of the microscope. It is thus possible to construct a 3D image of the sample by scanning voxel by voxel within the volume of interest. In FCM, the contrast and sensitivity of confocal microscopy is greatly enhanced as the fluorescent dye used to tag

chromatic aberrations, sample birefringence, index mismatches at dielectric interfaces along the light path. These and other effects can significantly worsen both axial and lateral resolution of FCM. For example, birefringent samples like liquid crystals cause the excitation beam to split into two separate beams which are focused at different spots, thus degrading the spatial resolution and making it dependent on the depth of imaging and sample birefringence.

Similar to conventional fluorescence microscopy (although we did not provide examples of this in the previous section), FCM enables multi-color imaging of sample composition patterns. Different constituents of the studied sample can be labeled with different dyes tailored to have different excitation and emission wavelengths and the resultant fluorescence patterns from each of them can be collocated to form separate images or overlaid to form a single multi-color image. For example, Figure 8(b) shows an image of phase-separated domains in a DNA/F-actin biopolymer mixture with the DNA and F-actin each labeled with a different dye [11]. Likewise, to obtain complementary information, one can use transmission mode bright field microscopy or polarizing microscopy, or a number of other optical imaging modalities to obtain images that can then be overlaid with the FCM images. This is demonstrated by an example of FCM textures [Fig. 8(c)] of a DNA pattern at the perimeter of dried drop overlaid with the PM image of the same sample area [12]. Multi-color imaging is especially useful in the study of composite soft matter systems.

Since imaging with a conventional confocal microscope is relatively slow, it is most often utilized in the study of stationary structures. To study dynamic processes in soft matter systems, researchers have recently started to utilize fast confocal microscopy

systems, which can be implemented by use of the fast laser scanning with acousto-optic deflectors (instead of galvano-mirrors) or using the Nipkow disc. One example of implementation of the fast confocal imaging system, shown in Fig. 9, employs a rotating Nipkow disc having thousands of pinholes, supplemented by a coaxial disc with micro-lenses. The two discs are mechanically connected and are rotated together by an electrical motor. The sample is scanned by thousands of excitation beams at once, and the resultant speed of FCM imaging is higher by orders of magnitude as compared to that of a conventional confocal microscope. The vertical refocusing is performed by a fast piezo z-stepper drive that is capable of an accurate (typically ~ 50 nm or better) vertical position setting. The speed of imaging can reach 100-1000 frames per second, although it depends on many factors, such as the needed contrast (i.e., the integration time of the fluorescence signal), size of the scanned area, and the frame-rate of the used CCD camera. Thus, Nipkow disc based FCM allows one to decipher dynamics of colloidal structures and other soft matter systems with up to millisecond temporal resolution. For example, fast FCM has been widely used to simultaneously localize multiple (millions) dye-marked particles and has provided deep insights into the physics of colloidal aggregation and phase transition in colloidal fluids, gels, glasses, etc. [13].

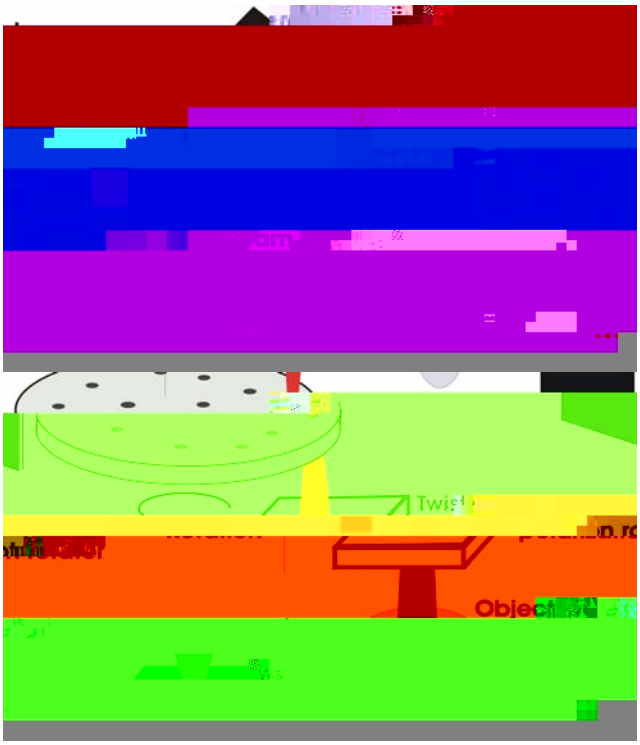

Figure 9. A schematic of Nipkow disc fluorescence confocal microscopy.

10.8. Fluorescence confocal polarizing microscopy

The FCM technique described above visualizes the distribution of fluorescent dye, providing insight into the spatial distribution of different dye-tagged constituents throughout the sample. The orientational order of anisotropic soft matter systems can be probed by combining conventional FCM with the capability of polarized light excitation and detection. In fluorescence confocal polarizing microscopy (FCPM) [10], this is commonly achieved by annexing the FCM setup with a polarization rotator introduced before the objective lens (Fig. 10), which enables controlled polarized excitation. In addition, FCPM requires that the specimen be stained with anisometric dye molecules which, on average, align parallel or perpendicular to the molecules of the studied “host” material. FCPM signal strongly depends on the angle between the transition dipole moment of the dye molecules and the polarization of excitation light. The intensity of fluorescence is maximized when the linear polarization of excitation light is parallel to the transition dipoles of excitation and fluorescence of the dye molecules in the sample,

axial direction, the scan is repeated at each axial depth. As a result, the resultant 3D image is comprised of a stack of thin (submicron) horizontal optical slices stored in the computer memory that can be then software-processed and presented in a variety of

(SFG) [17], third harmonic generation (THG) [18], and coherent Raman scattering, viz., coherent anti-Stokes Raman scattering (CARS) [19,20,21,22] and stimulated Raman scattering (SRS) [23,24].

Nonlinear optical microscopy has recently emerged as a powerful tool for non-invasive, label-free imaging with high 3D resolution capable of probing highly scattering thick biological and soft matter samples. In contrast to conventional single-photon excitation schemes (such as those used in fluorescence microscopy and ordinary Raman microscopy), the NLO signal is generated from nonlinear optical interactions involving multiple excitation photons. Hence, there are several advantages of using NLO microscopy as compared to conventional (linear) optical imaging: (1) low out-of-focus photobleaching (multi-photon absorption occurs only at the focus), (2) low photodamage (for example biological tissues absorb less in the near-infrared), (3) ability to excite ultra-violet (UV)-excitable fluorophores with visible or near-infrared light sources via two- or three-photon absorption, (4) inherent optical sectioning (no pinhole required because of a small excitation volume at the focal spot), (5) ability to work with thick specimens (larger penetration depth) and (6) chemical bond selectivity in coherent Raman imaging. However, nonlinear optical microscopy typically requires more expensive pulsed lasers

an optically excited nonlinear medium can be described by the induced polarization $P(t)$ expressed as a power series in electric field $E(t)$

picosecond pulsed laser is typically used as an excitation light source with wavelength in the near-infrared region. The intensity of the excitation light falls off inversely as the square of the axial distance from the focal plane and the efficiency of multi-photon absorption away from the focal point is extremely low because the probability of exciting

excitation pulses and the liquid crystal director **n**(**r**) as ~ $\cos^{2m}\beta$ for the detection with no polarizer and as ~ $\cos^{2(m+1)}\beta$ for imaging with the polarizer in the detection channel collinear with the polarization of the excitation beam, where m is the order of the nonlinear process (for example m=2 for two-photon excitation and m=3 for three-photon excitation [20,21,22]).

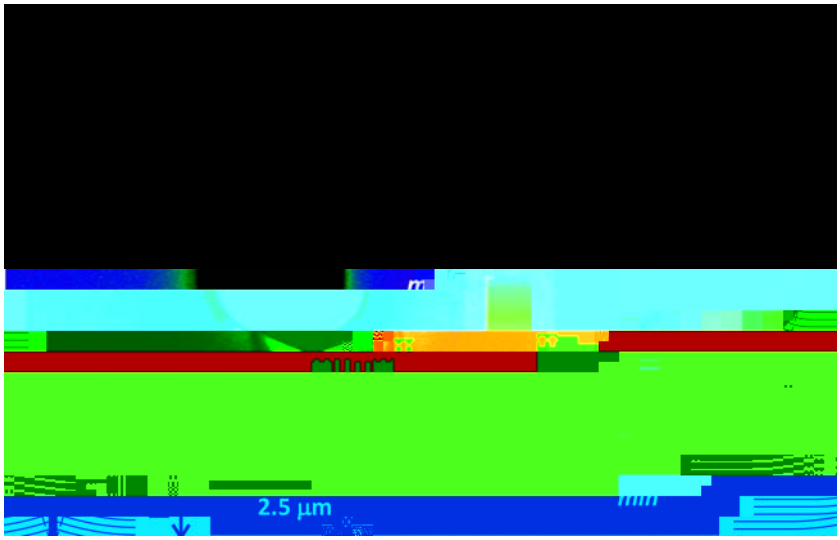

Figure 12. Application of multi-photon excitation fluorescence microscopy to imaging of a colloidal particle in a smectic liquid crystal. (a) Three-photon excitation fluorescence image of smectic liquid crystal layers deformations around a melamine resin sphere obtained with excitation at 870 nm and detection within 390~450 nm. (b) Reconstructed deformations of smectic layers around a spherical inclusion.

10.9.2. Multi-harmonic generation microscopy

The second- and third-harmonic generation microscopies derive contrast from variations in a specimen's ability to generate the respective harmonic signal from the incident light [16,17,18]. These multi-harmonic generation microscopies also require an intense laser light source (i.e., a pulsed laser). SHG signal emerging from the material is at exactly half the wavelength (frequency doubled) of the incident light interacting with the material via the second order nonlinear process. While two-photon excitation fluorescence is also a second order nonlinear process, it loses some energy during relaxation from the excited

state and, therefore, fluorescence occurs at wavelengths longer than half of excitation wavelength. In contrast, SHG process is energy conserving. The energy diagram of second and third harmonic generation processes [Fig. 11(b)] shows that there is no energy loss in the scattered light after multiple photons combine into a single photon of higher energy. In general, the setup for multi-harmonic generation microscopy is similar to that of multi-photon excitation fluorescence microscopy. Therefore, multi-harmonic generation imaging can be implemented with detection in the forward channel and simultaneously multi-photon excitation fluorescence imaging can be collected in the epi-detection channel, as shown in Fig. 11(c). SHG does not depend on excitation of fluorescent molecules. Hence it is not required to tag the specimen with a dye and the effects of photobleaching and photodamage are avoided. The second-order term $\chi^{(2)}$ in nonlinear process is nonzero only in media with no inversion symmetry while the $\chi^{(3)}$ term is nonzero for all media. Thus, imaging can also provide information about the symmetry of the studied materials by using these nonlinear processes.

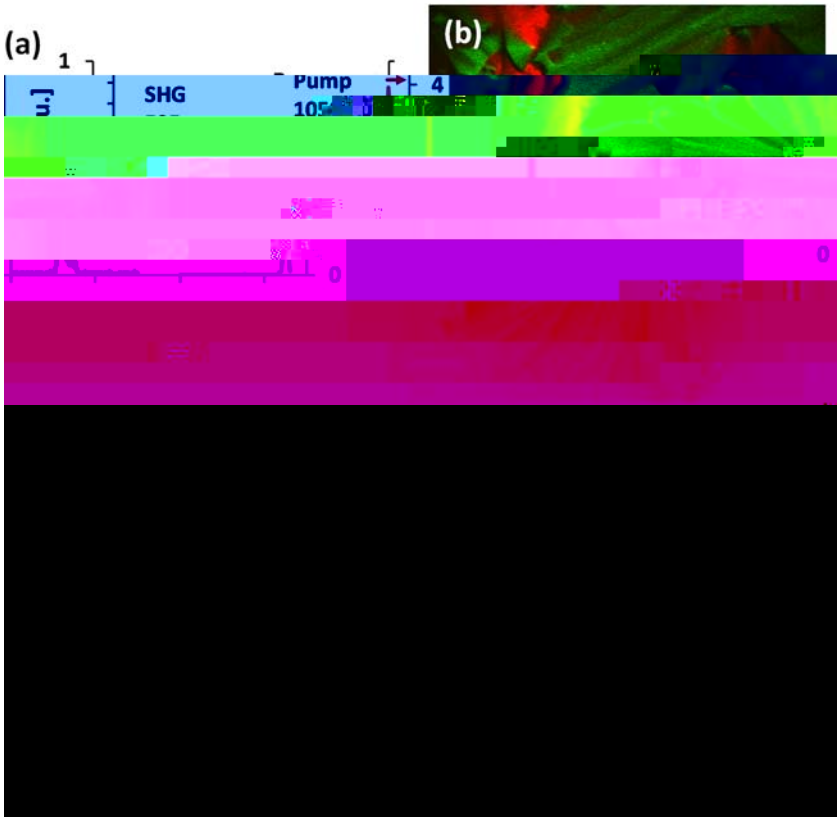
(a)
1
SHG
Pump
4
0
(b)

detected on the blue side, which is free from fluorescence interference, but it typically comes with a non-resonant background contribution.

The CARS technique utilizes a third order nonlinear process which involves three photons at two different frequencies called pump/probe ($\omega_p = \omega_{pump} = \omega_{probe}$) and Stokes ($\omega_s = \omega_{stokes}$) beams as shown in Fig. 14(a). When the frequency difference between the pump/probe and the Stokes beams matches a certain molecular vibrational frequency ($\omega_{vib} = \omega_p - \omega_s$) and the phase-matching condition of three input photons is fulfilled, a strongly enhanced blue-shifted anti-Stokes ($\omega_{as} = 2\omega_p - \omega_s$) resonance signal is generated

Similar to other NLO polarizing microscopy techniques, CARS polarizing microscopy exhibits a stronger sensitivity to spatial variations of the director **n**(**r**) as compared with the single-photon FCPM imaging.

As an example of the use of CARS polarizing microscopy technique, Figure 15(a,b) shows a vertical cross-section and in-plane images of a toric focal conic domain in a smectic liquid crystal thin film on a solid substrate. The signal due to CN-triple-bond vibration of the smectic liquid crystal (4-cyano-4'-octylbiphenyl, 8CB) provides information about the spatial pattern of the liquid crystal director. When the director is parallel to the polarization of excitation light, the intensity of the CARS signal is maximized, whereas the CARS intensity is minimized when the director is perpendicular to the polarization of incident light. The reconstructed structure of smectic layers in the toric focal conic domain is shown in Fig. 15(c), which was obtained using the 3D CARS images [Fig. 15(a,b)].

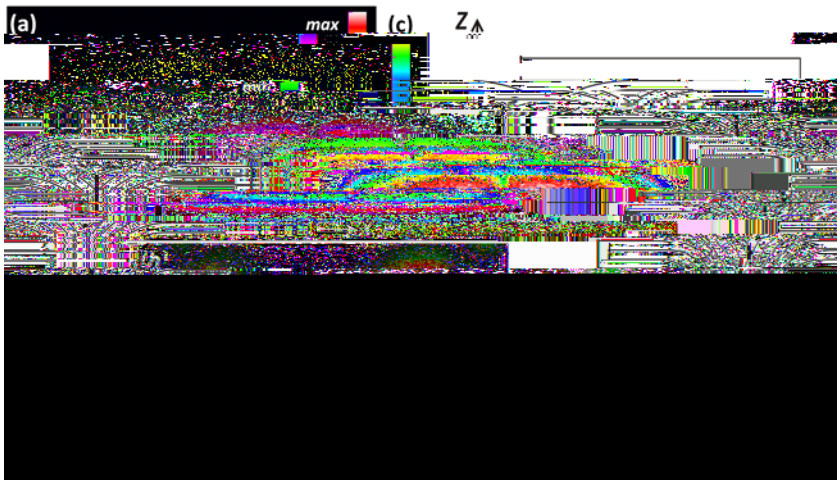

Figure 15. Coherent anti-Stokes Raman scattering images of toric focal conic domain in a smcetic liquid crystal thin film on a solid substrate. (a) Vertical cross-section and (b) in-plane images. (c) Reconstructed structure of smectic layers in the toric focal conic domain.

10.9.5. Stimulated Raman scattering microscopy

can be extended to enable orientation sensitive imaging by means of polarized excitation and detection.

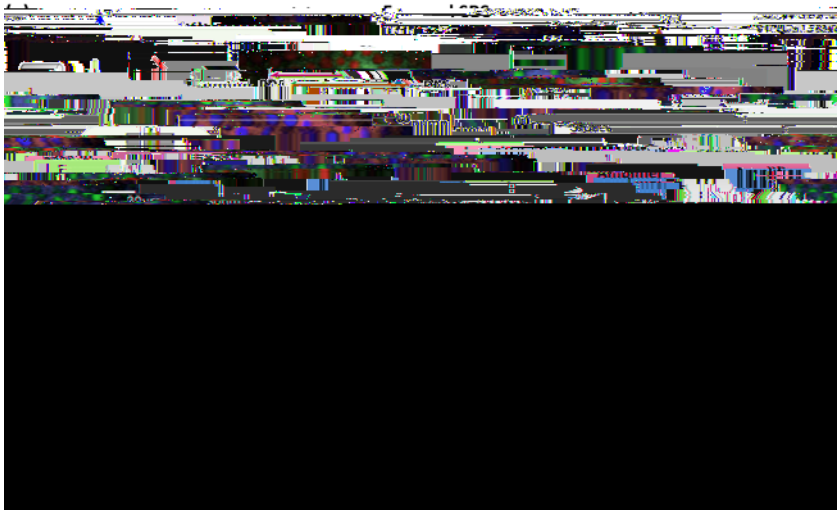

Figure 16. Stimulated Raman scattering microscopy. (a) Energy diagram and (b) detection scheme for SRS. Stokes beam is modulated at high frequency and the resulting amplitude modulation of the pump pulse (stimulated Raman loss) can be detected. (c) A schematic diagram for SRS microscope with forward SRS and epi CARS detection. (d) Two-color SRS image of DMSO (green) and lipid (red) in the subcutaneous fat layer. (image reprinted from [23] with permission from AAAS).

10.10. Three-dimensional localization using engineered point spread functions

Along with imaging of materials, high resolution tracking and localization of molecules and particles is helpful for understanding their self-assembly in soft matter systems. For instance, the image blurring caused by displacing the object away from the focal plane can be used as a rough measure in determining the axial position of an object in an image. One approach to localize an object in 3D with much finer resolution is to design the point spread function of the imaging system, as opposed to relying on the standard Airy disc PSF (Fig. 1c). Figure 17(a) shows an example of implementation of such an imaging system where the PSF is made up of two lobes that rotate as they traverse along the microscope's optical axis, forming a "double-helix" near the focal point [Fig. 17(b)]. The setup is built around a phase-mask at the Fourier plane in the imaging path, which can be

programmed by use of a spatial light modulator (SLM), as shown in Fig. 17(c) [25]. The SLM modulates the phase of the imaging beam at its Fourier plane, so that the resultant image of a particle captured by the CCD camera is presented in the form of two lobes. The axial position of an imaged particle is encoded as the angle of the line joining the lobes [Fig. 17(d)]. This technique can be used to localize scatterers (e.g., colloids) or fluorescent emitters (e.g., single fluorescent molecules) with the help of appropriate dichroic mirror and filters [Fig. 17(e)] achieving nanoscale resolution (typically ~10nm) in this spatial localization technique [26].

Figure 17. Optical imaging by use of engineered PSF. (a) Optical set-up for imaging with pre-engineered PSF. (b) Schematic representation of double-helix PSF. (c) Typical phase mask used to generate double helix-PSF. (d-e) Single molecule detection in 3D using double helix-PSF technique. (images from [25] copyright 2009 National Academy of Sciences, U.S.A.)

10.11. Integrating three-dimensional imaging systems with optical tweezers

Optical manipulation has proved to be of great importance in the study of colloidal systems, liquid crystals, and biological materials. Optical tweezers have been employed to study various liquid crystal systems, colloidal assemblies and interactions, as well as topology and structure of defects [27]. Manipulation of foreign inclusions and defects gives rise to a variety of director patterns in liquid crystals, which requires 3D imaging to fully understand their structures [14].

An integrated optical imaging and manipulation system, such as the one schematically depicted in Fig. 18(a), allows for simultaneous non-contact optical manipulation and imaging [28]. The optical manipulation employs a liquid crystal based SLM, which spatially modulates the phase of the inci0mp te1(nir bea9(od.he opase ofTJ0.0001 6c 0.011682

most frequently used not only in soft matter research but also in many other branches of science. Novel imaging approaches with improved resolution are especially needed to further the collective understanding of soft matter systems on the nanoscale. Several recently introduced approaches show the promise of providing significant breakthroughs in terms of overcoming resolution limits and may also be applied to the study of soft matter systems. In the future, their further development may allow for direct imaging of the self-assembly of molecules and nanoparticles and their condensed phase behavior.

Recently, a bulk of theoretical and experimental research has shown the feasibility of diffraction-unlimited optical imaging by use of simple optical elements based on metamaterials with a negative index of refraction. Theoretical works by Veselago [29] and Pendry [30], followed by numerous theoretical and experimental explorations, have demonstrated that the diffraction limit of conventional lenses is not a limiting factor for focusing of light by a lens made of a flat slab of metamaterial with a negative index of refraction, often referred to as a “super-lens” or a “perfect lens.” The improved resolution of the negative-index super-lens is due to the transmission of the evanescent surface waves, which are not lost (unlike in the case of conventional lenses). Being first considered theoretically over four decades ago by Veselago [29], metamaterials (also called “left-handed materials”) have never been encountered in nature or fabricated until the theoretical work of Pendry [30] provided important physical insights into how these unusual materials can be realized. Metamaterials are composed of structural units much smaller than the wavelength of incident light, so they appear homogeneous to the electro-magnetic waves. To obtain metamaterials with negative refractive index at optical frequencies, one has to achieve simultaneous “negative” electric and magnetic response

in the artificial nanofabricated composite material. Although the practical uses of metamaterials are still hindered by a number of technical challenges, such as losses, lenses and other optical elements made of metamaterials may one day revolutionize optical microscopy and enable nanoscale diffraction-unlimited imaging [31].

Several new techniques enabling sub-diffraction limited high-resolution optical imaging include near-field scanning optical microscopy (NSOM) [32], photoactivated localization microscopy (PALM) [33,34], and stochastic optical reconstruction microscopy (STORM) [35]. They can be extended for the study of soft matter systems, including the orientation-sensitive imaging of long-range molecular alignment patterns in liquid crystals. NSOM is a type of scanning probe microscopy for nanoscale investigation by observing the properties of evanescent waves. This is done by placing the probe very close to the sample surface. Light passes through a sub-wavelength diameter aperture and illuminates a sample that is placed within its near field, at a distance smaller than the wavelength of the light. With this technique, the resolution of the image is limited by the size of the detector aperture and not by the wavelength of the illuminating light. In particular, lateral resolution of 20 nm and vertical resolution of 2–5 nm have been demonstrated [32]. However NSOM is difficult to operate in a non-invasive mode and has a limited imaging depth.

The basic concept of PALM and STORM techniques is to fill the imaging area with many non-fluorescing fluorophores that can be photoactivated into a fluorescing state by a flash of light [33,34,35]. Since this photoactivation is stochastic, only a few, well-separated molecules can be detected and then localized by fitting the PSF with Gaussians with high precision. This process is repeated many times while photoactivating

different sets of molecules and building up an image molecule-by-molecule. The resolution of the final reassembled image can be much higher than that limited by diffraction. The demonstrated imaging resolution is 20 to 30 nm in the lateral dimensions and 50 to 60 nm in the axial dimension [36]. However the major problem with these emerging techniques is that it takes time on the order of hours to collect the data to get these high resolution images. Study of soft matter systems such as biological structures and colloidal nanoparticle dispersions will tremendously benefit from further development and use of these techniques.

In conjunction with high spatial resolution, imaging systems with high temporal resolution are required to study dynamic processes in soft-matter systems, for instance, the time-evolution of self-assembled structures, effect of applied external fields, etc. Nowadays, high-speed cameras with capture rates of up to a million frames per second are commercially available. There has been significant development on the front of enabling nonlinear, non-invasive optical imaging modalities like CARS and SRS to operate at video-rate, which will immensely benefit biological and soft matter systems research. This will eventually allow for in vivo optical imaging with molecular selectivity [37] and direct characterization of self-assemblies in composite systems.

advent of pulsed lasers has enabled implementation of nonlinear optical microscopies, furthering this trend and rendering the use of labeling agents unnecessary, while at the same time giving similar or better spatial resolution. NLO microscopy has also made it more convenient to image composite soft-matter systems by allowing imaging of different constituents in different nonlinear modalities simultaneously, instead of going through the difficult, and often impossible process of finding appropriate dyes that would bind to each of the constituents selectively. Further general development of optical microscopy techniques is an ongoing quest that will continue to contribute to the body of knowledge of soft matter systems.

References

1. Th. Jue, *Fundamental Concepts in Biophysics* (Humana Press, New York, 2009).
2. J. B. Pawley, *Handbook of Biological Confocal Microscopy,* 3rd ed. (Springer, New York, 2006).
3. N. H. Hartshorne and A. Stuart, *Crystals and the Polarising Microscope,* 4th ed (Edward Arnold (Publishers) Ltd., London, 1970).
4. Q. Liu, Y. Cui, D. Gardner, X. Li, S. He, and I. I. Smalyukh, *Nano Lett*. **10**, 1347 (2010).
5. F. D. Bloss,

25. D. B. Conkey, R. P. Trivedi, S.R.P. Pavani, I.I. Smalyukh, and R. Piestun, *Opt. Express* **19**, 3835 (2011).
26. S. R. P. Pavani, M. A. Thompson, J. S. Biteen, S. J. Lord, N. Liu, R. J. Twieg, R. Piestun, W. E. Moerner, *Proc. Natl. Acad. Sci. USA* **106**, 2995 (2008).
27. R. P. Trivedi, D. Engström, and I.I. Smalyukh, *J. Opt.* **13,** 044001 (2011).
28. R. P. Trivedi, T. Lee, K. Bertness, and I.I. Smalyukh, *Opt. Express* **18**, 27658 (2010).
29. V. G. Veselego,